HHS Public Access

Author manuscript

J Invest Dermatol. Author manuscript; available in PMC 2024 September 01.

Published in final edited form as:

J Invest Dermatol. 2024 September ; 144(9): 2029–2038. doi:10.1016/j.jid.2024.02.014.

CASZ1 Is Essential for Skin Epidermal Terminal Differentiation

Stephenie H. Droll[1], **Benny J. Zhang**[1], **Maxwell C. Levine**[1], **Celia Xue**[1], **Patric J. Ho**[1], **Xiaomin Bao**[1,2,3]

[1]Department of Molecular Biosciences, Weinberg College of Arts & Sciences, Northwestern University, Evanston, Illinois, USA

[2]Department of Dermatology, Feinberg School of Medicine, Northwestern University, Chicago, Illinois, USA

[3]Robert H. Lurie Comprehensive Cancer Center, Northwestern University, Chicago, Illinois, USA

Abstract

The barrier function of skin epidermis is crucial for our bodies to interface with the environment. Because epidermis continuously turns over throughout the lifetime, this barrier must be actively maintained by regeneration. Although several transcription factors have been established as essential activators in epidermal differentiation, it is unclear whether additional factors remain to be identified. In this study, we show that CASZ1, a multi zinc-finger transcription factor previously characterized in nonepithelial cell types, shows highest expression in skin epidermis. CASZ1 expression is upregulated during epidermal terminal differentiation. In addition, CASZ1 expression is impaired in several skin disorders with impaired barrier function, such as atopic dermatitis, psoriasis, and squamous cell carcinoma. Using transcriptome profiling coupled with RNA interference, we identified 674 differentially expressed genes with CASZ1 knockdown. Downregulated genes account for 91.2% of these differentially expressed genes and were enriched for barrier function. In organotypic epidermal regeneration, CASZ1 knockdown promoted proliferation and strongly impaired multiple terminal differentiation markers. Mechanistically, we found that CASZ1 upregulation in differentiation requires the action of both the master transcription factor, p63, and the histone acetyltransferase, p300. Taken together, our findings identify CASZ1 as an essential activator of epidermal differentiation, paving the way for future studies understanding of CASZ1 roles in skin disease.

Correspondence: Xiaomin Bao, Department of Molecular Biosciences, Weinberg College of Arts & Sciences, Northwestern University, 2205 Tech Drive, Hogan 2100, Evanston, Illinois 60208, USA. xiaomin.bao@northwestern.edu.

AUTHOR CONTRIBUTIONS

Conceptualization: SD, XB; Data Curation: SD, XB; Formal Analysis: SD, BZ, ML, CX; Funding Acquisition: SD, XB; Investigation: SD, BZ, ML, CX, PH; Methodology: SD, XB; Project Administration: XB; Resources: XB; Software: SD; Supervision: XB; Validation: SD, XB, Visualization: SD, XB; Writing - Original Draft Preparation: SD; Writing – Review and Editing: SD, XB

CONFLICT OF INTEREST

The authors state no conflict of interest.

SUPPLEMENTARY MATERIAL

Supplementary material is linked to the online version of the paper at www.jidonline.org, and at https://doi.org/10.1016/j.jid.2024.02.014.

Keywords

Barrier function; CASZ1; Differentiation; Keratinocytes; p63

INTRODUCTION

Epidermal barrier function is essential for protecting the human body from a host of environmental insults. Impaired barrier function contributes to a spectrum of skin disorders, including inflammation, infection, and cancer (Darido et al, 2016; Proksch et al, 2008). The epidermal barrier function is provided by the terminal differentiation process of keratinocytes (KCs). As skin epidermis continuously regenerates to compensate for wear and tear, a subset of progenitor-state KCs in the basal layer migrates toward the surface while undergoing biochemical and structural changes to form an enucleated, keratinized, and lipid-embedded barrier (Gonzales and Fuchs, 2017).

The activation of the epidermal terminal differentiation program is regulated at the transcriptional level. So far, several transcription factors essential for terminal differentiation have been identified, including GRHL3, KLF4, OVOL1, ZNF750, and the epidermal master transcription factor p63 (Bao et al, 2015; Boxer et al, 2014; Mardaryev et al, 2014; Nair et al, 2006; Segre et al, 1999; Soares and Zhou, 2018; Yu et al, 2006). It is unclear whether additional transcription factors critical for establishing the epidermal barrier remain to be identified.

CASZ1, a multi zinc-finger transcription factor, has previously been identified as an essential developmental regulator and activator of differentiation in T cells, nervous tissue, cardiac muscle tissue, and skeletal muscle tissue in model organisms (Christine and Conlon, 2008; Grosskortenhaus et al, 2006; Liu et al, 2014; Mattar et al, 2021; Mellerick et al, 1992). Expression of CASZ1 is tightly repressed or activated by lineage-specific transcription factors such as IKZF1 and PRRXL1 in neurons and MYOD/MYOG in muscle (Liu et al, 2020; Mattar et al, 2015; Monteiro et al, 2016). In cancer cell lines, the histone methyltransferase EZH2 and Ras-MAPK signaling mediate CASZ1 repression (Liu et al, 2020; Wang et al., 2012). However, the regulation of CASZ1 and its functions in epithelial tissue remains unknown.

In this study, we show that epidermal KCs, especially in the differentiated state, express high levels of CASZ1. CASZ1 knockdown significantly downregulates genes associated with KC terminal differentiation. In organotypic epidermal regeneration, CASZ1 knockdown promotes proliferation and impairs differentiation. Mechanistically, we show that both p63 and p300 bind at the CASZ1 locus and activate CASZ1 in KC differentiation. Interestingly, CASZ1 expression is impaired in multiple skin disorders. Taken together, our findings identified CASZ1 as an essential activator of epidermal terminal differentiation, downstream of p63 and p300, and that CASZ1 may be apreviously unreported driver or biomarker of skin disease.

RESULTS

CASZ1 is highly expressed in differentiated skin epidermal cells

CASZ1 has been previously characterized primarily in neural and muscle tissues, so we began by utilizing GTEx (Genotype-Tissue Expression) data to examine CASZ1 expression in various human tissues. Among all the tissues, CASZ1 expression was greatest in the skin. This expression is likely attributable to the epidermis because fibroblasts express minimal CASZ1 (Figure 1a). To confirm, we examined published single-cell RNA-sequencing data (Solé-Boldo et al, 2020; Wiedemann et al, 2023), which show that KCs express higher levels of CASZ1 than other cell types residing in skin. In addition, the terminally differentiating KCs (KRT14+, LOR+, FLG+, TGM1+) express higher levels of CASZ1 than other KCs (KRT14+, LOR−, FLG−, TGM1−) (Figure 1b). Next, we stained skin sections with a CASZ1 antibody and found that CASZ1 is prominently enriched in the nuclei of the suprabasal layers but not the basal layer near the dermis (Figure 1c). To further corroborate these observations, we subjected KCs to calcium-induced differentiation (Figure 1d) and examined both the CASZ1a and CASZ1b isoforms, which are produced by alternative splicing (Figure 1e). Consistent with the tissue staining pattern, undifferentiated KCs expressed little CASZ1, and both isoforms expressions increased significantly and progressively at both the mRNA (Figure 1f) and protein (Figure 1g and h) levels through day 2 and day 4 of differentiation. These data demonstrate that CASZ1 expression increases strongly during epidermal differentiation, suggesting that CASZ1 upregulation may play a role in the epidermal differentiation process.

CASZ1 expression is dysregulated in several types of skin diseases

Given CASZ1's upregulation in epidermal differentiation, we investigated whether CASZ1 expression is dysregulated in skin disorders associated with impaired barrier function. We searched the Gene Expression Omnibus database for paired nonlesional versus lesional RNA-sequencing studies and retrieved CASZ1 expression data for atopic dermatitis (Hu et al, 2023; Tsoi et al, 2020), psoriasis (Deng et al, 2022; Merleev et al, 2022; Swindell et al, 2015), and cutaneous squamous cell carcinoma (cSCC) (Srivastava et al, 2022; Wan et al, 2019). For atopic dermatitis, we retrieved 79 pairs of nonlesional and lesional biopsies, which disclosed significantly reduced CASZ1 expression in the lesions (68 of 79 pairs, 86%) (Figure 2a). For psoriasis, we retrieved data for 66 pairs of non-lesion and lesion biopsies, which also disclosed significantly reduced CASZ1 expression in the lesions (55/66 pairs, 83%) (Figure 2b). Finally, we retrieved 17 pairs of normal adjacent skin and cSCC, which disclosed significantly reduced CASZ1 expression in cSCC (16 of 17 pairs, 94%) (Figure 2c). These data show that impaired CASZ1 expression is associated with a spectrum of serious skin disorders.

CASZ1 knockdown impairs KC differentiation

To determine whether high CASZ1 expression is essential for epidermal differentiation, we knocked down CASZ1 with ON-TARGETplus siRNA SMARTpool and differentiated the KCs. We achieved significant reduction of both isoforms after differentiation (Figure 3a). Transcriptomic profiling identified 674 differentially expressed genes ($\log_2$ fold change ± 1, $P < .05$) (gene list is provided in Supplementary Table S1). Total of 91% of these genes were

downregulated (Figure 3b), indicating that CASZ1 primarily functions as a transcription activator in the epidermis. We utilized DAVID (Database for Annotation, Visualization and Integrated Discovery) gene ontology (GO) analysis on the downregulated genes, which revealed significant enrichment in pathways related to epidermal differentiation, such as keratinization and establishment of skin barrier (Figure 3c) (GO analysis is shown in Supplementary Table S2). Using RT-qPCR, we confirmed that CASZ1 knockdown significantly reduced expression of several genes required for barrier formation (Figure 3d). The validated genes include cell–cell junctions (*CDSN*, *TJP1*), structural proteins (*LCE1A*, *LCE3E*, and *SPRR2G*), and lipid transport (*SPNS2*) genes.

Our laboratory previously used transcriptomic profiling to identify 5128 genes whose expression significantly ($\log_2$ fold change ± 1, $P < .05$) changed between the progenitor and day 4 of differentiation. We compared the 674 genes altered by CASZ1 knockdown with the 5128 genes altered during normal in vitro differentiation and identified 415 shared genes (Figure 3e). A total of 290 (70%) of these shared genes were normally upregulated during differentiation but were downregulated by CASZ1 knockdown (Figure 3f). These genes were enriched for the various aspects of epidermal differentiation and barrier formation (Figure 3g) (GO analysis is presented in Supplementary Table S3). Altogether, the data suggest that CASZ1 knockdown strongly impairs expression of a subset of genes, which would normally be induced during terminal epidermal differentiation.

CASZ1 knockdown impairs epidermal terminal differentiation

To examine CASZ1 function in tissue, we organotypically regenerated epidermis with either CTRLi- or CASZ1i-treated KCs. Epidermal stratification occurred in both conditions. We began by confirming CASZ1 knockdown in organotypic culture conditions. Staining with CASZ1 antibody revealed a significant decrease in the percentage of CASZ1-positive nuclei in the CASZ1i tissue (Figure 4a and b). The epidermal differentiation process includes the cessation of proliferation. However, staining with Ki-67, a proliferation marker, disclosed a significantly increased percentage of Ki-67–positive nuclei (Figure 4c and d) in the CASZ1i condition. In addition, the epidermal thickness was significantly increased in the CASZ1i condition (Figure 4e and f), consistent with increased proliferation.

Next, we assessed a panel of epidermal differentiation markers. Staining with Nile Red, a lipophilic dye, disclosed a significantly reduced lipid barrier in CASZ1i tissue (Figure 4g and h). Likewise, the terminal differentiation markers and structural proteins, loricrin (Figure 4i and j), FLG (Figure 4k and l), and involucrin (Figure 4m and n) all disclosed significantly reduced staining in the CASZ1i tissue. Finally, CDSN, a component of differentiated cell–cell junctions also demonstrated significantly reduced staining in CASZ1i tissue (Figure 4o and p). These data indicate that CASZ1 reduction impairs epidermal barrier formation.

CASZ1 upregulation in differentiation requires p63 and p300

Previous studies indicate that CASZ1 is regulated by tissue-specific transcription factors (Liu et al, 2020; Mattar et al, 2015; Monteiro et al, 2016). p63 is the master epidermal transcription factor, so we investigated whether p63 regulates CASZ1. First, we utilized a short interfering approach to knock down p63 and induced differentiation. We achieved high

knockdown efficiency and observed significant reduction of both CASZ1 isoforms (Figure 5a). Next, we compared our CASZ1i RNA-sequencing data with previously published day 4 differentiation p63i RNA-sequencing data (Bao et al, 2015) and identified 194 shared genes (Figure 5b). These genes were primarily downregulated in both conditions (188 of 194 genes) (Figure 5c) and include differentiation markers that we validated in this study (Figure 5d). The 194 shared genes were highly enriched for GO terms related to KC differentiation (Figure 5e) (GO analysis is provided in Supplementary Table S4). These data suggest that p63 functions upstream of CASZ1 in epidermal differentiation.

Therefore, we investigated whether p63 directly regulates CASZ1. First, we examined p63 binding. We generated undifferentiated and day 4 of differentiation p63 chromatin immunoprecipitation-sequencing (ChIP-seq) libraries and observed an increase in the number of p63 peaks across the CASZ1 locus in the differentiated state. Consistent with CASZ1 activation, we observed a large increase of H3K27ac across the CASZ1 locus from undifferentiated to day 4 of differentiation. Increased acetylation suggests the action of a histone acetyltransferase. p63 is known to interact with p300, and this cooperation is known to promote KC differentiation (Bao et al, 2015; Katoh et al, 2019). We used published day 4 of differentiation p300 ChIP-seq data (Bao et al, 2015) and observed p300 binding in the differentiated state overlapping with p63 peaks within the first intron, including a peak that is stable between progenitors and day 4 of differentiation (highlighted in pink) and another peak that is unique to the differentiated state (highlighted in yellow) (Figure 5f). To confirm CASZ1's regulation by p300, we examined differentiated KCs treated with the p300 inhibitors A485 or C646 or DMSO control. We found that p300 inhibition resulted in significant reduction of both CASZ1 isoforms (Figure 5g). The data suggest that during differentiation, the activities of both p63 and p300 are required to activate CASZ1, which in turn promotes the terminal differentiation program.

DISCUSSION

In this study, we demonstrate that CASZ1 is a crucial transcription factor that participates in activating the epidermal terminal differentiation program. Previous work using early-stage mouse embryos (embryonic days 8.0–12.5) identified high CASZ1 expression in neuronal and cardiac tissue (Vacalla and Theil, 2002). Existing CASZ1 research predominantly centers on these nonepithelial tissues. Leveraging the GTEx survey of human adult tissues, we identified the highest level of CASZ1 expression in the skin. Consistent with previous studies in muscle, neuronal, and blood tissues (Bhaskaran et al, 2018; Christine and Conlon, 2008; Liu et al, 2020), we found that CASZ1 expression increases during epidermal differentiation and that reduced CASZ1 expression impairs terminal differentiation. Although previous studies report that CASZ1 both promotes tissue-specific differentiation and suppresses nonlineage genes in muscle and neurons (Liu et al, 2020; Mattar et al, 2021, 2018), we observed minimal evidence of CASZ1-mediated repression in KC differentiation with our knockdown strategy.

We found that p63 is required for CASZ1 upregulation in differentiation. This finding agrees with the previous findings in other cell types that CASZ1 expression is controlled by lineage-specific transcription factors (Liu et al, 2020; Mattar et al, 2015; Monteiro et al,

2016). We identified p63 cobinding with p300 in the first intron of CASZ1. Differentiated tissues and tissue-specific genes tend to preferentially utilize intronic enhancers (Borsari et al, 2021). Previous studies demonstrated that p300 interacts with p63 and promotes epidermal differentiation (Bao et al, 2015; Katoh et al, 2019). We also found H3K27ac in the differentiated state, suggesting a switch to an active chromatin state. We confirmed that p300 is required for CASZ1 activation. On the basis of these findings, we suggest that p63 and p300 cooperate at an intronic enhancer to activate CASZ1, which in turn induces terminal epidermal differentiation.

Several *CASZ1* variants have been linked to congenital heart disease and death in humans, where the inherited or de novo missense or frameshift variants act dominantly (Guo et al, 2019; Huang et al, 2016; Orlova et al, 2022). However, these dominant variants were not associated with skin disorders. These variants may prevent CASZ1 from interacting with binding partners such as TBX20, a transcription factor that is essential for cardiovascular development but is not expressed in skin epidermis (Kennedy et al, 2017). Furthermore, it is likely that the CASZ1 protein generated from the functional allele could be sufficient to maintain epidermal terminal differentiation but insufficient to sustain the mechanical demands on the heart.

In addition to heart disease, multiple studies have linked CASZ1 function to carcinogenesis. Most studies identified CASZ1 as a tumor suppressor in cancer types such as clear cell renal cell carcinoma, hepatocellular carcinoma, and ovarian cancer (Kim et al, 2019; Wang et al, 2018; Wu et al, 2016). In agreement with these findings, we found that CASZ1 expression is significantly reduced in cSCC. Two other common skin diseases, atopic dermatitis and psoriasis, are also associated with reduced CASZ1 expression. These diseases are associated with KC hyperproliferation and epidermal barrier disruption (Darido et al, 2016; Orsmond et al, 2021; Weidinger et al, 2018). Consistent with reduced CASZ1 in these skin disorders, we observed in our regenerated skin model that CASZ1 knockdown was sufficient to drive increased proliferation and impaired terminal differentiation. We suggest that CASZ1 represents an exciting target worth additional investigation because CASZ1 may represent a novel driver of skin disease, a disease biomarker, or even a therapeutic target.

This study primarily focused on functionally characterizing CASZ1 in human primary KCs and in epidermal tissue. Future work such as comparing the specific contributions of the 2 CASZ1 isoforms and determining the roles of nuclear localization signal and nuclear export signal sequences would advance our understanding of CASZ1 in epidermal differentiation at the molecular level. Although CASZ1a is expressed in both mouse and human, the 2 homologs only share 90% amino acid identity. In particular, the C-terminal region diverges and includes a stretch of 16 amino acids unique to mouse. Future work comparing the 2 homologs will be very interesting to determine if characterizing CASZ1 in mouse models can fully recapitulate its molecular actions in human skin epidermal homeostasis and in skin disorders.

MATERIALS AND METHODS

KC culture

The use of pooled primary human KCs for characterizing gene function is determined as "Not Human Research" by Northwestern University Institutional Review Board because no patient information is linked and identifiable from all our data, including the RNA-sequencing and ChIP-seq data deposited to Gene Expression Omnibus. Human epidermal KCs were isolated from fresh, deidentified foreskin (Northwestern Skin Biology & Diseases Resource-Based Center, Institutional Review Board number STU00009443). The deidentified foreskin specimens were considered discarded materials according to Institutional Review Board policy, thus patient consent was not required. KCs from at least 6 different donors were pooled and cultured in a 1:1 mixture of Keratinocyte-SFM (Life Technologies) and Medium 154 (Life Technologies). Differentiation was induced by seeding KCs at confluency with the addition of 1.2 mM calcium chloride. For inhibitor treatment, KCs were treated with p300 inhibitors, 1 μM A-485 or 10 μM C646, or DMSO during calcium-induced differentiation.

Nucleofection

Approximately 3 million KCs were electroporated with 1 nm control, CASZ1 (L-020764-02-0010, Horizon), or p63 short interfering RNA (sequence CGACAGUCUUGUACAAUUUUU, Horizon) using 4D Nucleofector (Lonza) and P3 Primary Cell 4D-Nucleofector X Kit (Lonza) according to manufacturer's instructions.

Western blot

KCs were lysed in urea buffer. A total of 30 μg of lysate was separated by SDS-PAGE before transfer to nitrocellulose membranes. Membranes were blocked with Intercept Protein Free Blocking Buffer (Li-COR Bioscience). Primary antibodies were incubated 1:1000 overnight at 4 °C. Secondary antibodies were incubated 1:10,000 for an hour at room temperature. Blots were scanned using Li-COR Odyssey (Li-COR Bioscience) and quantified with Image Studio (Li-COR Bioscience). Urea buffer contained 8 M urea, 10% BME, 65 mM CHAPS, 40 mM Tris, and 2.5 mM EDTA. Antibodies are listed in Supplementary Table S5.

Organotypic culture

Dermis was received from the New York Firefighters Skin Bank. Use of human dermis from deidentified donors has been approved by institutional review board. The bottom of the dermis was sealed with Matrigel (354234, Corning). A total of 750,000 cells were seeded per piece of dermis. Cultures were raised to liquid/air interface for 5 days. Tissue was embedded in optimal cutting temperature before sectioning. Tissue was fixed with an equal mixture of cold acetone and methanol for 6 minutes. Tissue was incubated overnight at 4 C with primary antibody. Tissue was washed 3 times with PBS. Secondary antibody was added for 2 hours. Tissue was washed twice with PBS and once with Hoechst for 5 minutes. For CDSN staining, antigen retrieval was performed for 30 minutes at 75 °C in 10 mM sodium citrate at pH 9 before blocking. For Nile Red staining, Nile Red (Sigma-Aldrich) was diluted to 2.5 μg/ml in 75% glycerol and 25% acetone and applied to formalin-fixed tissue for 10

minutes. Tissue was washed 2 times with PBS and once with Hoechst for 5 minutes. For H&E, tissue was counterstained with Mayer's Hematoxylin Solution (Sigma-Aldrich) and eosin. Images were taken on an Evos FL Auto 2 (Invitrogen) and quantified using ImageJ. For intensity measurements, the mean intensity of the stained area was quantified for 10 fields for each biological replicate. The epidermal thickness was measured left, right, and center for 10 fields per condition. Ki67– and CASZ1-positive nuclei were counted manually in 5 fields per biological replicate. Antibodies are listed in Supplementary Table S6.

RNA extraction and qRT-PCR

RNA was extracted using the Quick-RNA Miniprep Kit (Zymo Research) and reverse transcribed with the SuperScript VILO cDNA synthesis kit (Thermo Fisher Scientific). qRT-PCR was performed with PowerUp SYBR Green Master Mix (Thermo Fisher Scientific). Ct values were normalized to 18S. Graphs display mean and SD of 3 biological replicates with *t*-test and *P*-values. Primer sequences are listed in Supplementary Table S7.

RNA sequencing

RNA was extracted with the Quick-RNA MiniPrep kit with DNase I treatment (Zymo Research). Libraries were prepared with the NEBNext Ultra II Directional RNA Library Prep Kit for Illumina (New England BioLabs) and the NEBNext Poly(A) mRNA Magnetic Isolation Module (New England BioLabs). The Northwestern University NUSeq Core Facility produced single-end 50 base-pair reads on the Illumina HiSeq 4000.

Public genomics data

CASZ1 tissue-specific expression data were accessed from the GTEx Project. p300 ChIP-seq and p63i RNA-sequencing data from differentiated KCs were downloaded from GSE67382. Our laboratory previously published KC differentiation RNA-sequencing data available in GSE127223. CASZ1 expression data for atopic dermatitis (GSE193309 and GSE121212), psoriasis (GSE186063, GSE121212, and GSE67785), and cSCC (GSE191334 and GSE125285) were retrieved. Data were pairs of normal and diseased tissue. Disease data were combined from available studies and analyzed by paired t-tests. Single-cell RNA-sequencing data were downloaded from GSE130973 and GSE202352. The single-cell data were processed with Seurat (Hao et al, 2024). To identify cell clusters, we considered terminally differentiated KCs as keratin 14 positive, loricrin positive, FLG+, and TGM1+. Other KCs expressed KRT14 positive, loricrin negative, FLG−, and TGM1−. Fibroblasts clusters were PGDFRA+ and COL1A2+. Melanocyte clusters were tyrosine positive.

RNA-sequencing data analysis

The following analysis pipelines were performed using Nextflow (Di Tommaso et al, 2017). For RNA sequencing, quality control was performed using FastQC with adaptor trimming by Trimgalore. Reads were aligned to hg38 from University of California, Santa Cruz by STAR (Dobin et al, 2013). Salmon (Patro et al, 2017) quantified gene expression. Downstream analysis was performed in R using DESeq2 (Love et al, 2014) for differential expression analysis. Genes were considered differentially expressed if $\log_2$ fold change was at least ±1 and *P*-value < .05. GO using lists of differentially expressed genes analysis

was performed with DAVID (species: *Homo sapiens*, background: default *Homo sapiens*, input: differentially expressed gene list, analysis: Gene Ontology) with results considered significant if false discovery rate < 0.05 (Sherman et al, 2022).

ChIP-seq

KCs were fixed with 1% formaldehyde in PBS for 10 minutes and then quenched with 0.125 M glycine. Nuclei were extracted by a 15-minute incubation on ice in swelling buffer. Nuclei were lysed in RIPA buffer and disrupted with a 27-gauge needle before sonication with a Bioruptor Pico sonicator (undifferentiated, 7 rounds; differentiated, 14 rounds, where 1 round = 10 × 30 seconds ON, 30 seconds OFF) (Diagenode). Lysate was incubated overnight with H3K27ac (Active Motif 39034) or p63 (Cell Signaling Technology, number 13109) antibody and Protein G Dynabeads (Thermo Fisher Scientific). Beads were washed for 10 minutes with buffers A, B, and C. Beads were rinsed quickly 2 times with TE buffer. DNAwas eluted at 67 °C overnight. RNase A was added to eluate at 37 °C for 1 hour followed by proteinase K at 55 °C for 1 hour. DNAwas purified using the ChIP DNA Clean and Concentrator Kit (Zymo Research) and quantified with the Qubit dsDNA HS assay (Thermo Fisher Scientific). Libraries were prepped with NEBNext Ultra II DNA Library Prep Kit for Illumina (New England BioLabs) and sequenced at the Northwestern University NUSeq Core Facility as single-end 50 base pair reads on the Illumina HiSeq 4000.

Swelling buffer contained 0.1 M Tris, 10 mM potassium acetate, 15 mM magnesium acetate, 1% NP40. RIPA buffer contained 1% NP40, 0.5% sodium deoxycholate, 0.1% SDS, and 1 mM EDTA in PBS. Buffer A contained 50 mM Tris hydrogen chloride, 0.15 M sodium chloride, 1 mM EDTA, 0.1% SDS, 1% Triton X-100, and 0.1% sodium deoxycholate. Buffer B contained 50 mM Tris hydrogen chloride, 0.5 M sodium chloride, 1 mM EDTA, 0.1% SDS, 1% Triton X-100, and 0.1% sodium deoxycholate. Buffer C contained 50 mM Tris-hydrogen chloride, 1 mM EDTA, 1% NP-40, 1% sodium deoxycholate, and 0.5M lithium chloride). Elution buffer contained 10 mM Tris-hydrogen chloride, 0.3 M sodium chloride, 5 mM EDTA, and 0.5% SDS.

Analysis was conducted using Nextflow, FastQC, and Trimgalore as stated in the RNA-sequencing section. Reads were aligned to hg38 using BWA-MEM (Li, 2013[1]) with default parameters. Peaks were called using MACS2 (Zhang et al, 2008) with narrow peak calling. Bigwig files were created with BEDtools (Quinlan and Hall, 2010).

Supplementary Material

Refer to Web version on PubMed Central for supplementary material.

ACKNOWLEDGMENTS

XB is supported by National Institutes of Health R01 (AR07515), American Cancer Society Research Scholar Grant (RSG-21-018-01), Searle Leadership Fund, Northwestern Skin Disease Research Center Pilot & Feasibility Award, and Basic Insights Award by Northwestern Cancer Center. SD is supported by National Institutes of Health F31 (F31CA261114). Genomics data were generated by the Northwestern University NUSeq Core Facility. Skin specimens were provided by the Skin Biology & Diseases Resource-Based Center at Northwestern University.

[1]Li H. Aligning sequence reads, clone sequences and assembly contigs with BWA-MEM. arXiv 2013.

DATA AVAILABILITY STATEMENT

Datasets related to this article can be found at Gene Expression Omnibus accession GSE241873 (https://www.ncbi.nlm.nih.gov/geo/query/acc.cgi?acc=GSE241873).

Abbreviations:

ChIP-seq	chromatin immunoprecipitation-sequencing
cSCC	cutaneous squamous cell carcinoma
GO	Gene Ontology
KC	keratinocyte

REFERENCES

Bao X, Rubin AJ, Qu K, Zhang J, Giresi PG, Chang HY, et al. A novel ATAC-seq approach reveals lineage-specific reinforcement of the open chromatin landscape via cooperation between BAF and p63. Genome Biol 2015;16:284. [PubMed: 26683334]

Bhaskaran N, Liu Z, Saravanamuthu SS, Yan C, Hu Y, Dong L, et al. Identification of Casz1 as a regulatory protein controlling T helper cell differentiation, inflammation, and immunity. Front Immunol 2018;9:184. [PubMed: 29467767]

Borsari B, Villegas-Mirón P, Pérez-Lluch S, Turpin I, Laayouni H, Segarra-Casas A, et al. Enhancers with tissue-specific activity are enriched in intronic regions. Genome Res 2021;31:1325–36. [PubMed: 34290042]

Boxer LD, Barajas B, Tao S, Zhang J, Khavari PA. ZNF750 interacts with KLF4 and RCOR1, KDM1A, and CTBP1/2 chromatin regulators to repress epidermal progenitor genes and induce differentiation genes. Genes Dev 2014;28:2013–26. [PubMed: 25228645]

Christine KS, Conlon FL. Vertebrate CASTOR is required for differentiation of cardiac precursor cells at the ventral midline. Dev Cell 2008;14:616–23. [PubMed: 18410736]

Darido C, Georgy SR, Jane SM. The role of barrier genes in epidermal malignancy. Oncogene 2016;35:5705–12. [PubMed: 27041586]

Deng J, Leijten E, Nordkamp MO, Zheng G, Pouw J, Tao W, et al. Multi-omics integration reveals a core network involved in host defence and hyperkeratinization in psoriasis. Clin Transl Med 2022;12:e976. [PubMed: 36536476]

Di Tommaso P, Chatzou M, Floden EW, Barja PP, Palumbo E, Notredame C. Nextflow enables reproducible computational workflows. Nat Biotechnol 2017;35:316–9. [PubMed: 28398311]

Dobin A, Davis CA, Schlesinger F, Drenkow J, Zaleski C, Jha S, et al. STAR: ultrafast universal RNA-seq aligner. Bioinformatics 2013;29:15–21. [PubMed: 23104886]

Gonzales KAU, Fuchs E. Skin and Its regenerative powers: an alliance between stem cells and their niche. Dev Cell 2017;43:387–401. [PubMed: 29161590]

Grosskortenhaus R, Robinson KJ, Doe CQ. Pdm and Castor specify late-born motor neuron identity in the NB7–1 lineage. Genes Dev 2006;20:2618–27. [PubMed: 16980589]

Guo J, Li Z, Hao C, Guo R, Hu X, Qian S, et al. A novel de novo CASZ1 heterozygous frameshift variant causes dilated cardiomyopathy and left ventricular noncompaction cardiomyopathy. Mol Genet Genomic Med 2019;7:e828. [PubMed: 31268246]

Hao Y, Stuart T, Kowalski MH, Choudhary S, Hoffman P, Hartman A, et al. Dictionary learning for integrative, multimodal and scalable single-cell analysis. Nat Biotechnol 2024;42:293–304. [PubMed: 37231261]

Hu T, Todberg T, Ewald DA, Hoof I, Correa da Rosa J, Skov L, et al. Assessment of Spatial and Temporal Variation in the Skin transcriptome of Atopic Dermatitis by Use of 1.5 mm Minipunch Biopsies. J Invest Dermatol 2023;143:612–20.e6. [PubMed: 36496193]

Huang RT, Xue S, Wang J, Gu JY, Xu JH, Li YJ, et al. CASZ1 loss-of-function mutation associated with congenital heart disease. Gene 2016;595:62–8. [PubMed: 27693370]

Katoh I, Maehata Y, Moriishi K, Hata RI, Kurata SI. C-terminal α domain of p63 binds to p300 to coactivate β-catenin. Neoplasia 2019;21: 494–503. [PubMed: 30986748]

Kennedy L, Kaltenbrun E, Greco TM, Temple B, Herring LE, Cristea IM, et al. Formation of a TBX20-CASZ1 protein complex is protective against dilated cardiomyopathy and critical for cardiac homeostasis. PLoS Genet 2017;13: e1007011. [PubMed: 28945738]

Kim B, Jung M, Moon KC. The prognostic significance of protein expression of CASZ1 in clear cell renal cell carcinoma. Dis Markers 2019;2019:1342161. [PubMed: 31481981]

Liu Z, Li W, Ma X, Ding N, Spallotta F, Southon E, et al. Essential role of the zinc finger transcription factor Casz1 for mammalian cardiac morphogenesis and development. J Biol Chem 2014;289:29801–16. [PubMed: 25190801]

Liu Z, Zhang X, Lei H, Lam N, Carter S, Yockey O, et al. CASZ1 induces skeletal muscle and rhabdomyosarcoma differentiation through a feed-forward loop with MYOD and MYOG. Nat Commun 2020;11:911. [PubMed: 32060262]

Love MI, Huber W, Anders S. Moderated estimation of fold change and dispersion for RNA-seq data with DESeq2. Genome Biol 2014;15:550. [PubMed: 25516281]

Mardaryev AN, Gdula MR, Yarker JL, Emelianov VU, Poterlowicz K, Sharov AA, et al. p63 and Brg1 control developmentally regulated higher-order chromatin remodelling at the epidermal differentiation complex locus in epidermal progenitor cells [published correction appears in Development 2014;141:3437] Development 2014;141:101–11. [PubMed: 24346698]

Mattar P, Ericson J, Blackshaw S, Cayouette M. A conserved regulatory logic controls temporal identity in mouse neural progenitors. Neuron 2015;85:497–504. [PubMed: 25654255]

Mattar P, Jolicoeur C, Dang T, Shah S, Clark BS, Cayouette M. A Casz1-NuRD complex regulates temporal identity transitions in neural progenitors. Sci Rep 2021;11:3858. [PubMed: 33594190]

Mattar P, Stevanovic M, Nad I, Cayouette M. Casz1 controls higher-order nuclear organization in rod photoreceptors. Proc Natl Acad Sci USA 2018;115:E7987–96. [PubMed: 30072429]

Mellerick DM, Kassis JA, Zhang SD, Odenwald WF. castor encodes a novel zinc finger protein required for the development of a subset of CNS neurons in Drosophila. Neuron 1992;9:789–803. [PubMed: 1418995]

Merleev A, Ji-Xu A, Toussi A, Tsoi LC, Le ST, Luxardi G, et al. Proprotein convertase subtilisin/kexin type 9 is a psoriasis-susceptibility locus that is negatively related to IL36G. JCI Insight 2022;7:e141193. [PubMed: 35862195]

Monteiro CB, Midão L, Rebelo S, Reguenga C, Lima D, Monteiro FA. Zinc finger transcription factor Casz1 expression is regulated by homeodomain transcription factor Prrxl1 in embryonic spinal dorsal horn late-born excitatory interneurons. Eur J Neurosci 2016;43:1449e59. [PubMed: 26913565]

Nair M, Teng A, Bilanchone V, Agrawal A, Li B, Dai X. Ovol1 regulates the growth arrest of embryonic epidermal progenitor cells and represses c-myc transcription. J Cell Biol 2006;173:253–64. [PubMed: 16636146]

Orlova A, Guseva D, Ryzhkova O. Identification of a novel de novo variant in the CASZ1 causing a rare type of dilated cardiomyopathy. Int J Mol Sci 2022;23:12506. [PubMed: 36293425]

Orsmond A, Bereza-Malcolm L, Lynch T, March L, Xue M. Skin barrier dysregulation in psoriasis. Int J Mol Sci 2021;22:10841. [PubMed: 34639182]

Patro R, Duggal G, Love MI, Irizarry RA, Kingsford C. Salmon provides fast and bias-aware quantification of transcript expression. Nat Methods 2017;14:417–9. [PubMed: 28263959]

Proksch E, Brandner JM, Jensen JM. The skin: an indispensable barrier. Exp Dermatol 2008;17:1063–72. [PubMed: 19043850]

Quinlan AR, Hall IM. BEDTools: a flexible suite of utilities for comparing genomic features. Bioinformatics 2010;26:841–2. [PubMed: 20110278]

Segre JA, Bauer C, Fuchs E. Klf4 is a transcription factor required for establishing the barrier function of the skin. Nat Genet 1999;22:356–60. [PubMed: 10431239]

Sherman BT, Hao M, Qiu J, Jiao X, Baseler MW, Lane HC, et al. David: a web server for functional enrichment analysis and functional annotation of gene lists (2021 update). Nucleic Acids Res 2022;50:W216–21. [PubMed: 35325185]

Soares E, Zhou H. Master regulatory role of p63 in epidermal development and disease. Cell Mol Life Sci 2018;75:1179–90. [PubMed: 29103147]

Solé-Boldo L, Raddatz G, Schütz S, Mallm JP, Rippe K, Lonsdorf AS, et al. Single-cell transcriptomes of the human skin reveal age-related loss of fibroblast priming. Commun Biol 2020;3:188. [PubMed: 32327715]

Srivastava A, Tommasi C, Sessions D, Mah A, Bencomo T, Garcia JM, et al. MAB21L4 deficiency drives squamous cell carcinoma via activation of RET. Cancer Res 2022;82:3143–57. [PubMed: 35705526]

Swindell WR, Remmer HA, Sarkar MK, Xing X, Barnes DH, Wolterink L, et al. Proteogenomic analysis of psoriasis reveals discordant and concordant changes in mRNA and protein abundance. Genome Med 2015;7:86. [PubMed: 26251673]

Tsoi LC, Rodriguez E, Stölzl D, Wehkamp U, Sun J, Gerdes S, et al. Progression of acute-to-chronic atopic dermatitis is associated with quantitative rather than qualitative changes in cytokine responses [published correction appears in J Allergy Clin Immunol 2023;151:1413] J Allergy Clin Immunol 2020;145:1406–15. [PubMed: 31891686]

Vacalla CM, Theil T. Cst, a novel mouse gene related to Drosophila Castor, exhibits dynamic expression patterns during neurogenesis and heart development. Mech Dev 2002;118:265–8. [PubMed: 12351199]

Wan J, Dai H, Zhang X, Liu S, Lin Y, Somani AK, et al. Distinct transcriptomic landscapes of cutaneous basal cell carcinomas and squamous cell carcinomas. Genes Dis 2019;8:181–92. [PubMed: 33997165]

Wang C, Liu Z, Woo CW, Li Z, Wang L, Wei JS, et al. EZH2 Mediates epigenetic silencing of neuroblastoma suppressor genes CASZ1, CLU, RUNX3, and NGFR. Cancer Res 2012;72:315–24. [PubMed: 22068036]

Wang JL, Yang MY, Xiao S, Sun B, Li YM, Yang LY. Downregulation of castor zinc finger 1 predicts poor prognosis and facilitates hepatocellular carcinoma progression via MAPK/ERK signaling. J Exp Clin Cancer Res 2018;37:45. [PubMed: 29506567]

Weidinger S, Beck LA, Bieber T, Kabashima K, Irvine AD. Atopic dermatitis. Nat Rev Dis Primers 2018;4:1. [PubMed: 29930242]

Wiedemann J, Billi AC, Bocci F, Kashgari G, Xing E, Tsoi LC, et al. Differential cell composition and split epidermal differentiation in human palm, sole, and hip skin. Cell Rep 2023;42:111994. [PubMed: 36732947]

Wu YY, Chang CL, Chuang YJ, Wu JE, Tung CH, Chen YC, et al. CASZ1 is a novel promoter of metastasis in ovarian cancer. Am J Cancer Res 2016;6:1253–70. [PubMed: 27429842]

Yu Z, Lin KK, Bhandari A, Spencer JA, Xu X, Wang N, et al. The Grainyhead-like epithelial transactivator Get-1/Grhl3 regulates epidermal terminal differentiation and interacts functionally with LMO4. Dev Biol 2006;299:122–36. [PubMed: 16949565]

Zhang Y, Liu T, Meyer CA, Eeckhoute J, Johnson DS, Bernstein BE, et al. Model-based analysis of ChIP-Seq (MACS). Genome Biol 2008;9:R137. [PubMed: 18798982]

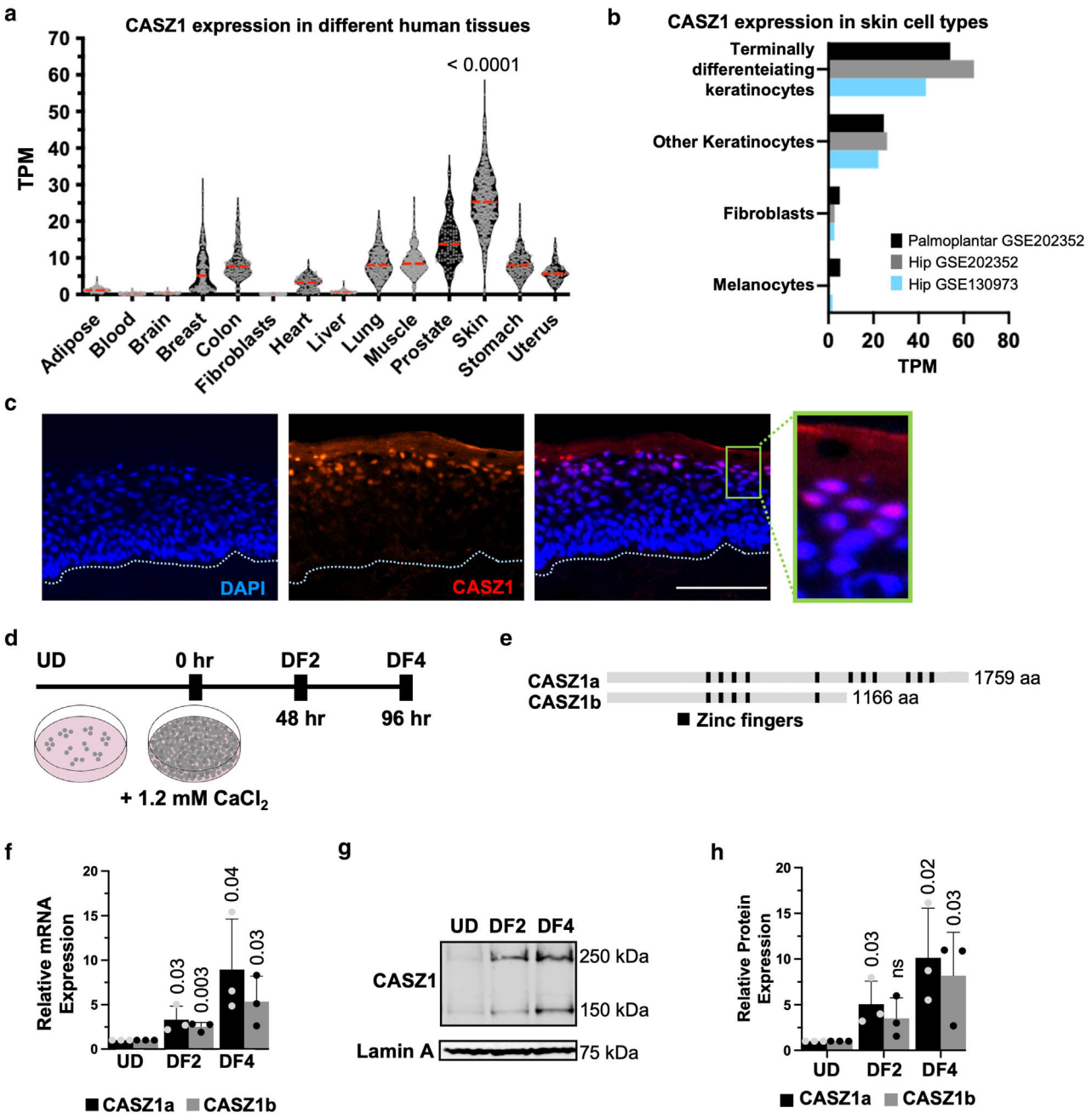

Figure 1. CASZ1 expression increases during epidermal differentiation.

(**a**) GTEx mRNA expression data showing that *CASZ1* expression is significantly greater in skin than in other human tissues. Red lines denote medians. One-way ANOVA was used. (**b**) Single-cell RNA-sequencing data showing CASZ1 expression in skin-resident cell types in palmoplantar and hip skin samples. (**c**) Representative images of CASZ1 staining in the skin. CASZ1 is detectable in the differentiated layers of epidermal tissue. Dotted line indicates the basement membrane. The area in green box is enlarged to the far right to show CASZ1 and DAPI colocalization. White bar indicates 125 μm. (**d**) Diagram showing the time points used in keratinocyte differentiation time course for CASZ1 expression

analyses. (**e**) Diagram showing the CASZ1a and CASZ1b protein isoforms. (**f**) RT-qPCR showing the relative CASZ1a and CASZ1b expression during keratinocyte differentiation. Student's *t*-tests (UD vs DF2 and UD vs DF4) were used. Mean ± SD of 3 biological replicates are shown. (**g**) Representative western blot showing increasing expression of both CASZ1 isoforms during differentiation. (**h**) Quantification of western blots. Student's *t*-tests (UD vs DF2 and UD vs DF4) were performed. Mean ± SD of 3 biological replicates are shown. DF2 and DF4 denote day 2 and day 4 of differentiation, respectively. UD denotes undifferentiated. $CaCl_2$, calcium chloride; GTEx, Genotype-Tissue Expression; hr, hour; TPM, transcripts per million.

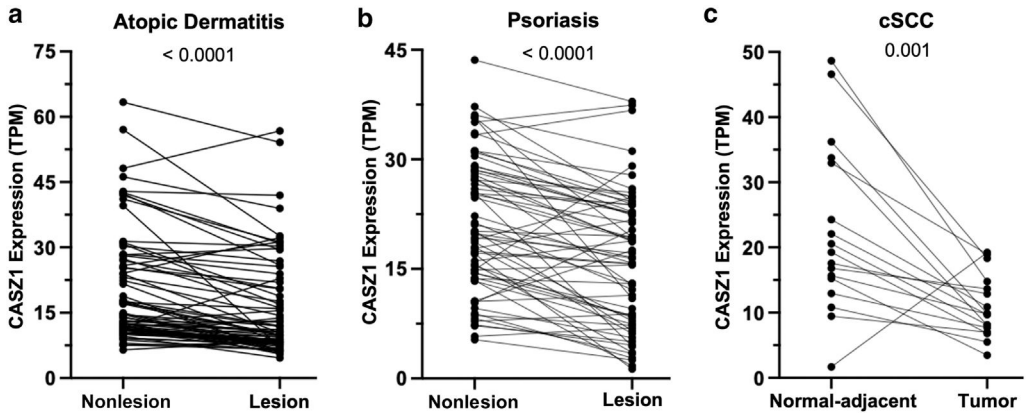

Figure 2. CASZ1 expression is dysregulated in several types of skin diseases.

(**a**) Paired expression data from nonlesional and lesional skin from patients with atopic dermatitis. Paired *t*-test was performed. (**b**) Paired expression data from nonlesional and lesional skin from patients with psoriasis. Paired *t*-test was performed. (**c**) Paired expression data from normal-adjacent skin and cSCC tumors. Paired *t*-test was performed. cSCC, cutaneous squamous cell carcinoma; TPM, transcripts per million.

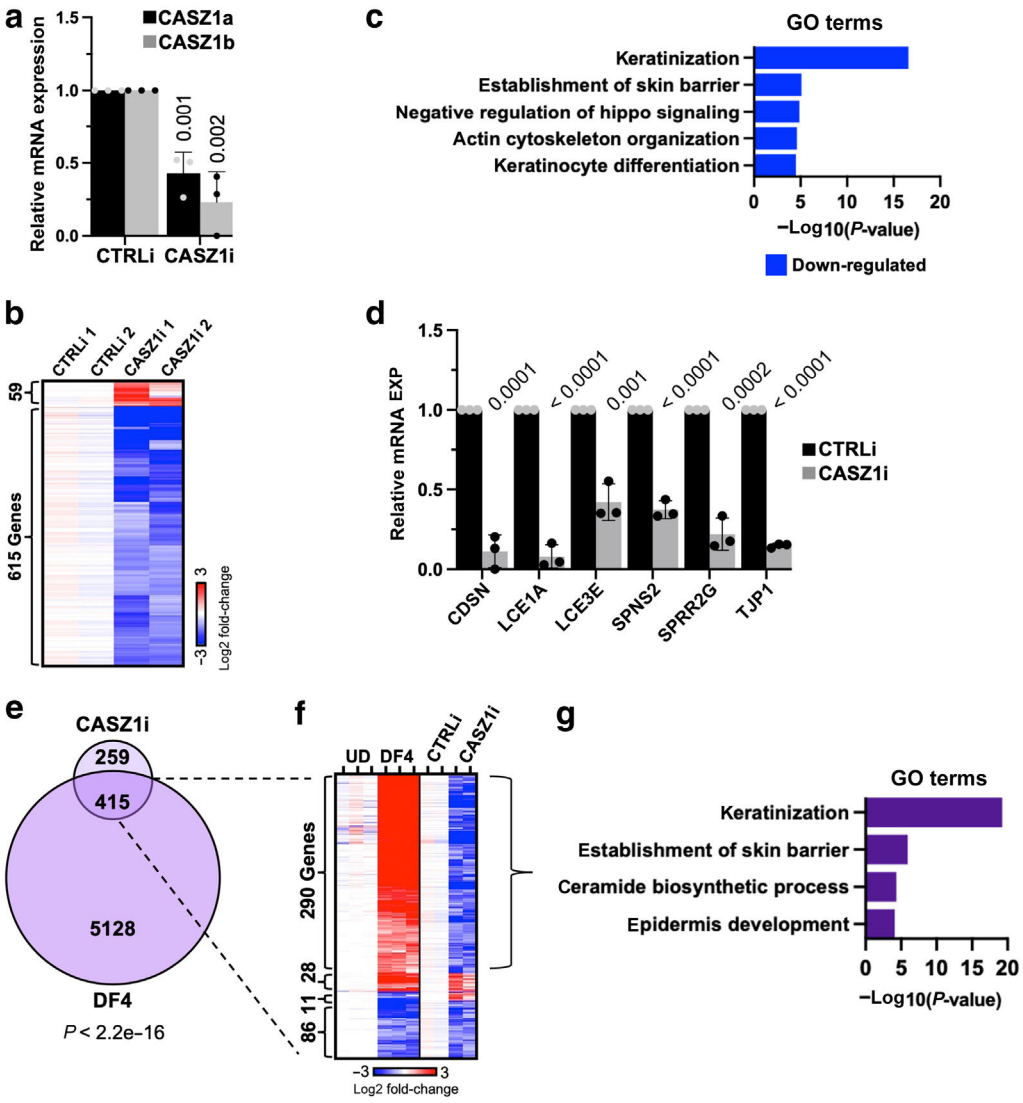

Figure 3. CASZ1 knockdown impairs keratinocyte differentiation.

(**a**) RT-qPCR showing CASZ1 knockdown efficiency in differentiated keratinocytes after siRNA treatment. Mean ± SD of 3 biological replicates are shown. Student's *t*-tests. (**b**) Heatmap showing differentially expressed genes ($\log_2$ fold change > 1, $P < .05$) by RNA-seq in the differentiated state after siRNA treatment. (**c**) GO terms derived from differentially expressed genes. (**d**) RT-qPCR validation of RNA sequencing confirming decreased expression of epidermal differentiation markers. Mean ± SD of 3 biological replicates are shown. Student's **t**-tests were performed. (*e*) Identification of genes differentially expressed in both calcium induced differentiation and CASZ1 siRNA treatment. Fisher's exact test was performed. (**f**) Heatmap showing the relative expression of the 415 shared genes from CASZ1i and differentiation RNA-seq data sets. (**g**) GO terms of 290 shared genes of interest. UD denotes undifferentiated, and DF4 denotes day of differentiation. GO, Gene Ontology; RNA-seq, RNA sequencing; siRNA, small interfering RNA.

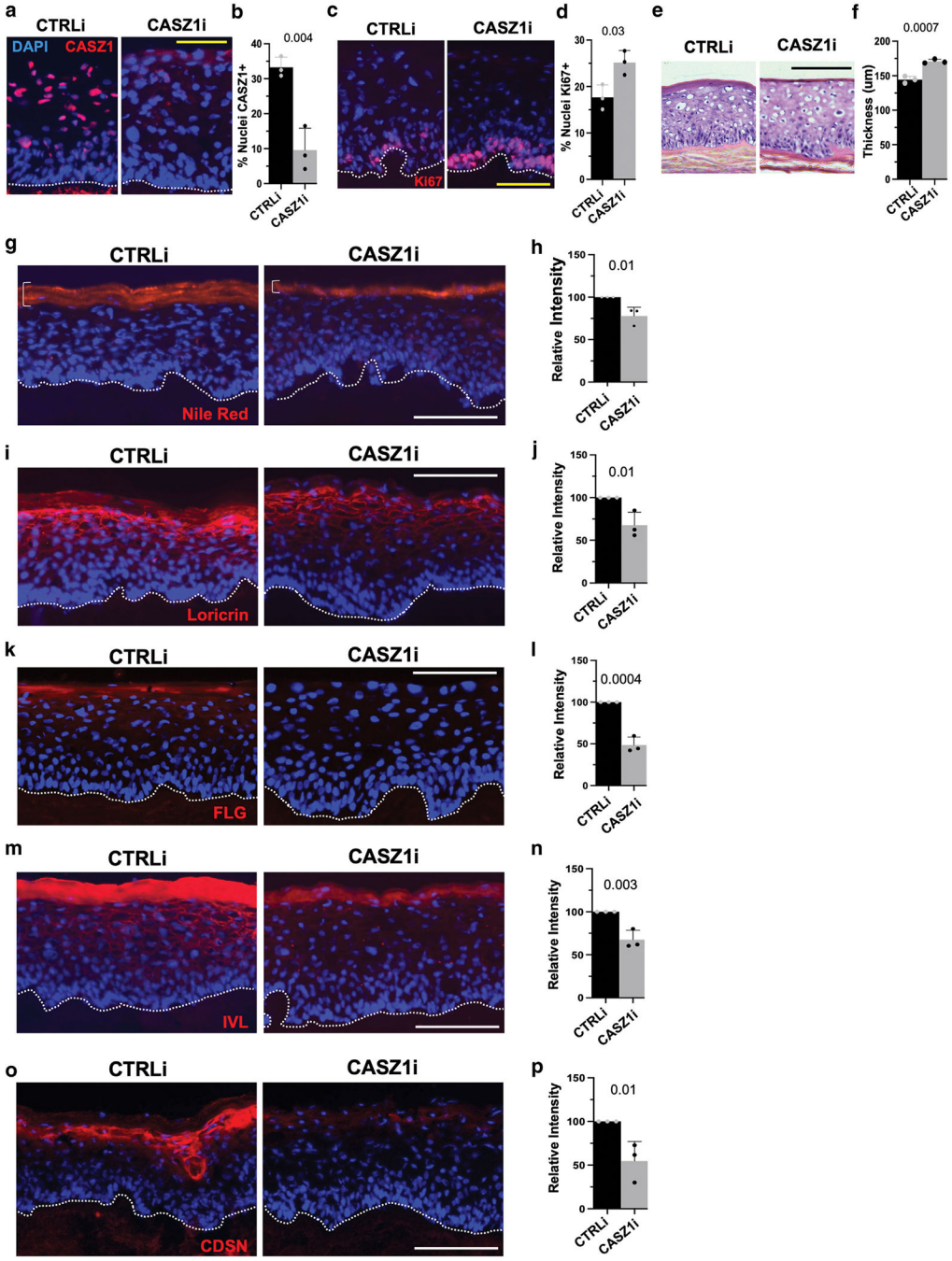

Figure 4. CASZ1 knockdown impairs epidermal terminal differentiation.

(**a**) Representative images of CASZ1 staining in control and CASZ1 siRNA organotypic cultures. Dotted white lines indicate basement membrane for all images in this figure. All yellow bars = 75 μm. (b) Quantification of the percentage of nuclei that are positive for CASZ1 expression. All graphs in this figure display mean ± SD of 3 biological replicates with student's *t*-tests. (**c**) Representative images of Ki-67 staining. (**d**) Quantification of the percentage of nuclei that are positive for Ki-67 expression. (**e**) Representative H&E images. Black bar = 150 μm. (**f**) Quantification of epidermal thickness. (**g**) Representative images

of Nile red staining. White brackets indicate epidermis with positive Nile red staining. All white bars = 125 μm. (**h**) Quantification of Nile red intensity. (**i**) Representative images of loricrin staining. (**j**) Quantification of loricrin intensity. (**k**) Representative images of FLG staining. (**l**) Quantification of FLG intensity. (**m**) Representative images of involucrin staining. (**n**) Quantification of involucrin intensity. (**o**) Representative images of CDSN staining. (**p**) Quantification of CDSN intensity. siRNA, small interfering RNA.

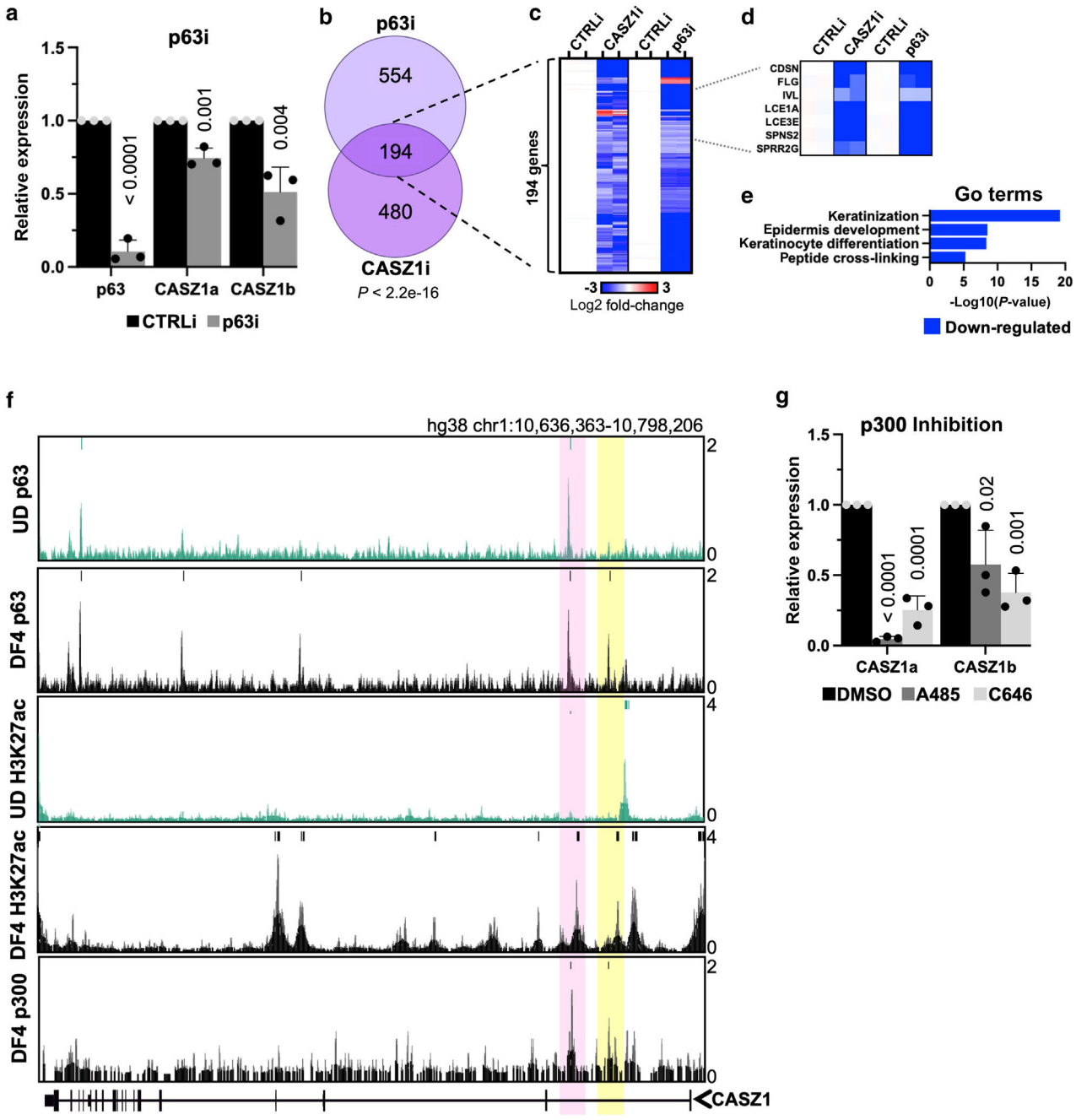

Figure 5. CASZ1 upregulation in differentiation requires p63 and p300.

(**a**) RT-qPCR showing p63 knockdown efficiency in differentiated keratinocytes and CASZ1 expression in response to p63i. Mean ± SD of 3 biological replicates with student's *t*-tests are shown. (**b**) Overlap of differentially expressed genes *p63i* and *CASZ1i* RNA-seq data sets. Fisher's exact test. (**c**) A heatmap of the differentially expressed genes shared by CASZ1i and p63i. (**d**) A zoom in of the heatmap showing epidermal differentiation markers validated in this study. (**e**) Top GO terms of the 194 shared genes. (**f**) The pink and yellow highlights indicate the regions of interest. Genome browser tracks at the CASZ1 locus showing p63 binding in intron 1 overlapping with increased H3K27ac and p300 peaks in

DF4. (**g**) RT-qPCR showing decreased CASZ1 expression in response to p300 inhibitor treatments. Mean ± SD of 3 biological replicates with student's *t*-tests are shown. DF4, day 4 of differentiation; GO, Gene Ontology; RNA-seq, RNA-sequencing.